ANALYSIS OF RHODAMINE AND FLUORESCEIN-LABELED F-ACTIN DIFFUSION IN VITRO BY FLUORESCENCE PHOTOBLEACHING RECOVERY

JOHN R. SIMON,* ALBERT GOUGH,* ELSE URBANIK,‡ FEI WANG,‡ FREDERICK LANNI,* BENNIE R. WARE,‡ AND D. L. TAYLOR*

*Center for Fluorescence Research in Biomedical Sciences, Carnegie-Mellon University, Pittsburgh, Pennsylvania 15213; and ‡Department of Chemistry, Syracuse University, Syracuse, New York 13244

ABSTRACT Properties of filamentous acetamidofluorescein-labeled actin and acetamidotetramethylrhodamine-labeled actin (AF and ATR-actin, respectively) were examined to resolve discrepancies in the reported translational diffusion coefficients of F-actin measured in vitro by FPR and other techniques. Using falling-ball viscometry and two independent versions of fluorescence photobleaching recovery (FPR), the present data indicate that several factors are responsible for these discrepancies. Gel filtration chromatography profoundly affects the viscosity of actin solutions and filament diffusion coefficients. ATR-actin and, to a lesser degree, AF-actin show a reduction in viscosity in proportion to the fraction labeled, presumably due to filament shortening. Actin filaments containing AF-actin or ATR-actin are susceptible to photoinduced damage, including a covalent cross-linking of actin protomers within filaments and an apparent cleavage of filaments detected by a decrease of the measured viscosity and an increase in the measured filament diffusion coefficients. Quantum yields of the two photoinduced effects are quite different. Multiple cross-links are produced relative to each photobleaching event, whereas <1% filament cleavage occurs. Substantial differences in the filament diffusion coefficients measured by FPR are also the result of differences in illumination geometry and sampling time. However, under controlled conditions, FPR can be used as a quantitative tool for measuring the hydrodynamic properties of actin filaments. Incremented filament shortening caused by photoinduced cleavage or incremental addition of filament capping proteins produces a continuous and approximately linear increase of filament diffusion coefficients, indicating that filaments are not associated in solution. Our results indicate that actin filaments exhibit low mobilities and it is inferred that actin filaments formed in vitro by column-purified actin, under standard conditions, are much longer than has conventionally been presumed.

INTRODUCTION

The diffusion coefficients of F-actin in vitro have been measured previously by a variety of methods that have yielded contradictory results. Measurements by quasielastic light scattering have indicated diffusion coefficients of $\sim 10^{-8}$ cm^2/s (Carlson and Frazer, 1974; Janmey et al., 1986), measurements by periodic-pattern modulation-detection fluorescence photobleaching recovery (periodic-pattern FPR) have yielded diffusion coefficients of 10^{-9}–10^{-10} cm^2/s (Lanni and Ware, 1984; Mozo-Villarias and Ware, 1984), and other investigators using gaussian spot fluorescence photobleaching recovery (spot FPR) reported diffusion coefficients of $<10^{-10}$ (Tait and Frieden, 1982*a*) and $\ll 2 \times 10^{-11}$ cm^2/s (Tait and Frieden, 1982*b*) or no measurable recovery over the time course of the experiment. These discrepancies have also contributed to a controversy involving rheometry of actin. Viscoelastic properties of actin filaments have been interpreted as a result of self association of actin filaments into a static gel network (Sato et al., 1985) or an opposing theory based on topological constraints of long actin filaments without self association (Zaner and Stossel, 1983; Ito et al., 1987). The former theory predicts that in general, actin filaments are immobile, whereas the latter predicts that actin filaments have a finite mobility (diffusion coefficient) albeit slower than that predicted for noninteracting rigid rods in solution.

This study addresses some of the basic issues related to the use of FPR in defining actin filament hydrodynamics. These issues include actin purity, properties of fluorescent analogues of actin, and instrumental parameters including the total dose and geometry of illumination. We have found that acetamidofluoresceinyl-actin (AF-actin) and acetamidotetramethylrhodamine-actin (ATR-actin) are susceptible to photodamage as assayed by falling ball viscometry, cross-linking detected by SDS-gel electrophoresis, and by FPR depending on the protocol of measurement. In addition, the purity of actin after gel filtration can

Address correspondence to John R. Simon, Department of Biology, University of North Carolina, CB #3280, 433 Wilson Hall, Chapel Hill, NC 27599-3280.

profoundly affect the diffusion coefficient of filaments and the apparent viscosities. The understanding of these issues should lead to improved criteria for experimental design and for the interpretation of actin filament properties.

MATERIALS AND METHODS

Materials

Trizma base (Tris), ethylene glycol bis(B-aminoethyl ether)-*N,N'*-tetra-acetic acid (EGTA), sodium azide, phenylmethylsulfonyl fluoride (PMSF), 1,4-piperazinediethanesulfonic acid (Pipes), glutathione (reduced form), bovine serum albumin, and phalloidin were from Sigma Chemical Co. (St. Louis, MO); adenosine triphosphate (ATP) and dithiothreitol (DTT) were from Boehringer-Mannheim (Indianapolis, IN); rhodamine-phalloidin was from Molecular Probes, Inc. (Junction City, OR); and all other chemicals were from J. T. Baker Chemical Co. (Philipsburg, NJ).

Actin

Rabbit skeletal muscle actin was purified from the acetone powder according to the MacLean-Fletcher and Pollard (1980*a*) modification of Spudich and Watt (1971), and was stored lyophilized in 2 mg sucrose/mg actin. Lyophilized actin was resuspended and dialyzed verses buffer A (2 mM Tris, 0.5 mM ATP, 0.2 mM DTT, 0.1 mM $CaCl_2$, 0.02% azide, 75 mg/liter PMSF, pH 8 at 4°C), then clarified by centrifugation at 100,000 *g* for 1.5 h at 4°C. We term this actin as "S&W-actin" (Spudich and Watt actin) to signify the method of preparation, and to note that the actin was not column purified at this point. The acetamidofluoresceinyl (AF-actin) and acetamidotetramethylrhodamine (ATR-actin) fluorescent actin analogues were prepared by a method based on Wang and Taylor (1980) and Tait and Freiden (1982*a*) as follows. Approximately 3–4 ml of S&W-actin (~5 mg/ml) were polymerized by bringing the solution to 100 mM KCl and 2 mM $MgCl_2$ and allowing it to set for 1 h at 23°C. For the acetamidofluorescein-actin labeling reaction, 2.4 mg of 5'-iodoacetamidofluorescein (5'-IAF; Molecular Probes, Inc.) were dissolved in 100 μl dimethylsulfoxide per 10 mg actin to give a 20× molar excess of dye per actin. The dye was then dissolved into borate buffer (100 mM borate, 100 mM KCl, 2 mM $MgCl_2$, pH 8.5 at 23°C) of equal volume per volume to the actin by dropwise addition with stirring, on ice. This solution was added to the polymerized actin and homogenized by trituration, then allowed to react for 1 h in the dark at 23°C. The reaction was quenched by adding DTT to 2 mM. The ATR-actin labeling reaction was similar to the AF-actin except 0.68 mg of 5'(-6')-iodoacetamidotetramethylrhodamine (IATR; Molecular Probes, Inc.) was dissolved in 100 μl of *N,N'*-dimethylformamide to give a 5× molar excess of dye per actin, and the reaction was allowed to proceed 2 h on ice. The following steps apply to both AF- and ATR-actin. The actin solution was centrifuged as above to sediment the F-actin, and the pellet was briefly rinsed with buffer A. The pellet was resuspended in 2–4 ml of buffer A, allowed to soften for 2–4 h, then gently homogenized in a glass-Teflon homogenizer. The resulting solution was dialyzed overnight vs. 2 liters of buffer A to complete the depolymerization. The solution was centrifuged as above and applied to a 1.5 × 100 cm column of Sephacryl S300 (Pharmacia, Inc., Piscataway, NJ) equilibrated in buffer A. The actin eluted at ~90 ml elution volume (flow rate = 14 ml/h) and the pooled fractions were polymerized and depolymerized twice more by the method described above. The final dialysis was against buffer C (2 mM Pipes, 0.5 mM ATP, 0.2 mM DTT, 0.02% sodium azide, 75 mg/l PMSF, 0.1 mM $CaCl_2$, pH 7.0 at 23°, and degassed). The extent of labeling was determined according to Simon and Taylor (1986). The extinction coefficient used for fluorescein was 60,000 $M^{-1}cm^{-1}$ at 495 nm according to Wang and Taylor (1980) and for rhodamine was 49,340 $M^{-1}cm^{-1}$ at 560 nm (see below). Yields were ~50% from the AF-actin labeling, and ~25% for the ATR-actin labeling at a dye/protein ratio of 0.5–1.0 for both. Unlabeled, column purified actin (CP-actin) was purified by S300 chromatography (see Results) as above, followed by one round of polymerization and depolymerization.

For the periodic-pattern FPR experiments, performed in the Syracuse laboratory, actin was prepared and labeled according to previously reported procedures (Plank and Ware, 1986, 1987; Mozo-Villarias and Ware, 1985) except actin was chromatographed on a 2.5 × 50 cm Sephadex G-150 column both before and after labeling. Actin was stored at 4°C for not longer than 5 d as G-actin in continuous dialysis against buffer G (2 mM Tris, 0.2 mM $CaCl_2$, 0.2 mM DTT, 0.02% azide, pH 8.0) with changes of fresh buffer at least daily. Before experimentation actin samples were required to meet two criteria using periodic-pattern FPR: (*a*) the diffusion coefficient of G-actin was required to exceed 7.0×10^{-7} cm^2/s (excluding the possibility of significant oligomerization) and (*b*) the extent of assembly upon addition of standard assembly medium (to 2 mM Mg^{+2}, 100 mM KCl) was required to meet or exceed control values for the actin concentration employed (excluding the possibility of significant nonassembly-competent actin or of actin assembly inhibitors).

Determination of Extinction Coefficients

The extinction coefficient for ATR-actin was determined as follows. Between 3–5 mg of IATR (Molecular Probes, Inc.) was accurately weighed and dissolved into buffer C (less DTT). The peak absorbance (552 nm) was used to calculate the molar extinction coefficient of IATR in this buffer. The spectra of IATR and ATR-actin in 2% SDS, 4 M urea, and with cysteine conjugated to the IATR in buffer C were compared. Under all of these conditions the molar extinction coefficients did not significantly change, and spectral peaks shifted at most 3 nm. Therefore the extinction coefficient at the peak absorbance of IATR (552 nm) was used as an estimate for the extinction coefficient of ATR-actin at its peak absorbance (560 nm). The spectral properties of IATR purchased from Research Organics, Inc. (Cleveland, OH) were examined in the same manner and in addition the IATR was partially purified as follows. Approximately 5 mg of IATR was dissolved in borate buffer, loaded onto a Sep-Pak C_{18} column (Waters Associates, Milford, MA), and the column was washed with several volumes of water. The dye was step eluted with methanol, vacuum dried, and analyzed.

Sample Preparation

G-actin in buffer C was polymerized by the addition of a 10× stock solution to bring the final buffer conditions in all experiments to 20 mM Pipes, 100 mM KCl, 1 mM ATP, 2 mM $MgCl_2$, 1 mM EGTA, 0.98 mM $CaCl_2$ (~pCa 5), pH 7 at 23°. To obtain various percents labeled actin, an appropriate amount of unlabeled actin was added to either the AF or ATR-actin. Protein concentrations were determined by the method of Bradford (1976) using reagent purchased from Pierce Chemical Co. (Rockford, IL). BSA ($E^{1\%}_{280} = 6.6$) and actin ($E^{1\%}_{290} = 6.2$) were used as standards.

Falling Ball Viscometry

Falling ball viscometry (FBV) has been described previously by MacLean-Fletcher and Pollard (1980*b*) and Pollard and Cooper (1982). Briefly, samples were drawn into 100-μl glass capillaries and the ends were sealed with modeling clay. The samples were incubated at 23°C for 2 h, then assayed. A stainless steel sphere (0.025", The Micro Ball Company, Peterborough, NH) was inserted into the capillary and the time for the sphere to fall a fixed distance at an angle of 30, 60, or 80° was measured. Viscosities were determined by linear interpolation of inverse velocities of standard glycerol solutions of known viscosities given by Fowler and Taylor (1980) and Fowler and Pollard (1982). Because actin solutions are viscoelastic non-Newtonian fluids, the data are reported as apparent viscosities.

In some experiments, the FBV capillary was "irradiated" as follows. The sample capillary was masked with a felt-tip marker or electrical tape

to leave four 1-cm exposed areas separated by 1.5-cm-wide masks. The capillary was placed into a holder and a laser beam expanded to a 1.5-cm-diameter gaussian spot was centered on a 1-cm exposed area of the capillary. In some cases a cylindrical lens was placed before the sample to focus the gaussian spot into a rectangle approximately the width of the capillary (2 mm). This increased the effective laser illumination density ~10-fold. The light power was measured at the sample using a laser power meter.

Gaussian Spot Fluorescence Photobleaching Recovery (Spot FPR)

The theory and method of gaussian spot FPR have been described previously (Axelrod et al., 1976). The instrument is essentially the same as that described by Koppel et al. (1976), except as noted. An argon ion laser (model 2020; Spectra Physics, San Jose, CA) was operated at 488 nm for AF-actin samples and 514 nm for ATR-actin samples. In order to critically align the monitoring and bleaching beams, a small optical wedge was positioned between the beam-splitting optical flats, in the path of the attenuated (monitoring) beam. Neutral density filters (Melles Griot, Irvine, CA) were mounted between the beam expander and the microscope to attenuate the laser beam as necessary. The gaussian beam entered a Zeiss Universal microscope through an epi-illuminator (Zeiss IIIRS) equipped with fluorescein and rhodamine filter sets. The beam was focused to ≈2.0 μm spot size (w) in the specimen using a 40× (0.75 N.A.) Zeiss Neofluor objective. A 0.4-mm aperture was placed in the secondary image plane to limit the observation depth of field to ~19 μm (Tait and Frieden, 1982*b*), or 1/10 the thickness of the capillary. Fluorescence was monitored using a single photon counting system consisting of a photomultiplier tube (943G; Hamamatsu, Middlesex, NJ) mounted in a thermoelectrically cooled housing (TE104RF; Products for Research, Danvers, MA) maintained at −40°C, and connected to a photon counter (Thorn EMI Gencom Inc., Plainview, NY). The instrument was interfaced to an IBM PC-AT, which controlled the shuttering sequence, the counting intervals, and data acquisition from the photon counter. Spot size (w) was measured by translating a 50-μm-diameter aperture through the magnified image (≈200 μm diameter), in 12.7-μm steps, and fitting a gaussian curve to the measured intensity profile. Spotsize (w) was taken as the radius at $1/e^2$ intensity. Samples were prepared as described above and loaded into 200-μm path length flat capillaries (Vitro Dynamics, Rockaway, NJ) which were sealed and fixed to black anodized aluminum flats using FloTexx (Lerner Laboratories, New Haven, CT). The samples were incubated for 2 h at ambient temperature (22–24°C) then assayed. The total illumination dose to the sample was minimized during measurement by attenuating and shuttering the laser beam. AF-Actin measurements were typically made with the laser light power at 300 mW and a 3.0 OD neutral density filter in the optical path, whereas ATR-actin measurements were made at 400 mW laser power, and 2.3 OD neutral density filter. The FPR bleaching beam intensities were typically 657 and 2,920 W/cm^2 for AF- and ATR-actin, respectively. Power measurements were made on defocused beams using a laser power meter (820; Newport Research Corp., Fountain Valley, CA), with the sensor located below the microscope objective. In all measurements the specimen was illuminated for 240 ms periods, spaced at intervals that started at 1 s and increased in duration by 1.1-fold each time. During each illumination period two 100-ms counts were recorded. Thus data points were more closely spaced early in the record when the intensity had the greatest rate of change, and illumination was minimized in the latter part of the record when intensity was changing more slowly. Multiple recovery curves were acquired under identical conditions and averaged to increase the signal-to-noise ratio. The averaged data were then analyzed by the method of Yguerabide et al. (1982) on an IBM PC-AT.

To test the effect of illumination on the diffusion of the labeled actin, capillaries were "preirradiated" by rotating the nosepiece of the epi-illuminator to an open position, removing or changing the neutral density filters, and exposing the capillary to the 2-mm-diameter gaussian unfocused laser beam. The objective was then rotated back into position, and a photobleaching measurement made as described above.

Periodic-Pattern, Modulation-Detection FPR (Periodic-Pattern FPR)

The translational diffusion coefficient of AF-actin was also measured by periodic-pattern, modulation-detection FPR (periodic-pattern FPR). The theory and design of the apparatus have been described (Lanni and Ware, 1982), and applications to actin assembly and mobility in vitro and in vivo have been reported (Lanni and Ware, 1984; Mozo-Villarias and Ware, 1984, 1985; Plank and Ware, 1986, 1987; Wang et al.; 1982). Briefly, a periodic pattern was bleached onto the sample by brief (100–300 ms) intense illumination through a grating using a gaussian beam (70 μm radius at the sample) from an argon ion laser (λ = 488 nm). The grating was then linearly translated at constant speed to create a moving excitation pattern on the sample. As the translating grating moves into and out of phase with the bleached pattern on the sample, an AC component of the detector photocurrent is created. For a single diffusing species, the AC modulation envelope (E) of the detector signal decays as an exponential given by: $E(t)/E(0) = e^{-Dk^2t}$ + constant. D is the translational diffusion coefficient of the fluorescent tracer and k (6,381 cm^{-1}) is the wave vector magnitude given by: $k = 2\pi/L$, where L (9.85 μm) is the periodicity of the grating pattern on the sample. The pattern was formed by imaging a 300 line/inch Ronchi ruling through a 16× objective. Modulation decays were typically monitored for 1–5 min. In some experiments the modulation decay was monitored for much longer times (up to 3 h) using intermittent measurements spaced by longer periods of time during which the monitor beam was blocked to prevent photodamage. Actin samples were polymerized in 100-μm-pathlength flat capillaries (Vitro Dynamics) and were incubated for at least 1 h before measurements were made. All data were fit to the equation above or, in the case of very slow recoveries, to a linearized representation of the initial slope.

Sedimentation

Actin sedimentation was used to examine byproducts of light irradiation of labeled actin. The samples were prepared as above but drawn into 200-μl glass capillary tubes. The samples were then irradiated by focusing a 1.5 × 0.2 mm rectangular beam onto the capillary, and the capillary was mechanically translated at an oscillatory velocity of 14 cm/s to expose the entire capillary. The capillary was then broken open into a centrifuge tube and allowed to incubate an additional hour, after which it was sedimented in an airfuge (Beckman Instruments Inc., Fullerton, CA) at 23 psi for 15 min (100,000 *g*). The supernatant was drawn off, protein concentration was measured by the Bradford assay, and the pellet was resuspended in gel sample buffer containing 2% SDS and 250 mM 2-mercaptoethanol. Samples of the supernatant and pellet were run on SDS-PAGE, stained with Coomassie Blue, and quantitated using a gel scanner (E-C Apparatus Corp., St. Petersburg, FL).

RESULTS

Preparation of ATR-Actin

The absorbance spectrum of ATR-actin prepared as described in the materials and methods (Fig. 1) differs from the previously reported spectrum (Tait and Frieden, 1982*a*), mainly due to the absence in our preparation of the strong absorbance peak at ~360 nm. In addition, we measured a molar absorptivity coefficient of 49,340 $M^{-1}cm^{-1}$ for ATR-actin compared with previous values of 24,000 and 23,000 $M^{-1}cm^{-1}$ (Taylor et al., 1981; Tait and Frieden, 1982*a*). The previous authors used IATR pur-

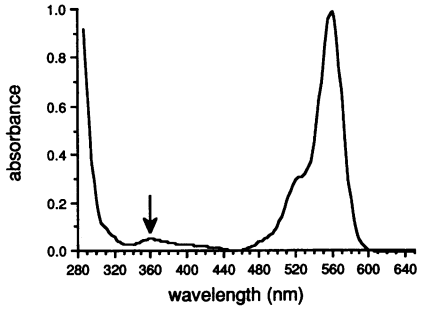

FIGURE 1 Absorbance spectrum of ATR-actin. The absorbance spectrum of ATR-actin labeled at a dye/protein ratio of 1.0 in buffer C was taken. The arrow indicates a small absorption peak at 360 nm which may be due to a reactive contaminant in the 5'-IATR dye (see Results).

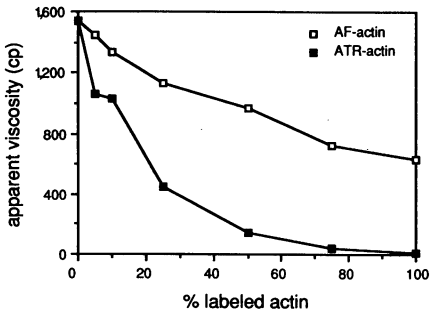

FIGURE 2 Low-shear falling ball viscometry (FBV) of AF- and ATR-actin. AF and ATR-actin were mixed with appropriate amounts of unlabeled actin to give the indicated fraction labeled actin. The actin was polymerized at 0.5 mg/ml under the following buffer conditions: 20 mM Pipes, 100 mM KCl, 1 mM ATP, 2 mM $MgCl_2$, pCa~5, and pH 7 at 23°C. After 2 h incubation at 23°C the viscosity of the solution was measured by FBV (see Material and Methods). Each point represents the average of three measurements.

chased from Research Organics, Inc., Cleveland, OH. We measured the absorbance spectra of IATR from this supplier and indeed a strong absorbance peak at 360 nm was present (data not shown), which was absent from the dye used in these studies (Molecular Probes, Inc.). To determine if the 360 nm absorbance was due to the dye or a contaminant, we partially purified the dye by binding the dissolved dye onto a hydrophobic column (see Materials and Methods), washing the column with water, then eluting the bound dye with methanol. A slightly yellowish compound was eluted by the water, which had a strong absorbance at 360 nm but no absorption between 400 and 600 nm. The partially purified rhodamine dye, eluted by the methanol, had an approximate twofold reduced absorbance at 360 nm relative to the 552 nm peak, signifying that the 360 nm peak was due to an impurity.

AF vs. ATR-Actin

The viscosities measured by FBV of fluorescently labeled actin (AF- and ATR-actin) are shown in Fig. 2. As the fraction of labeled actin was increased (by adding labeled actin to unlabeled, column-purified actin) the apparent low shear viscosity decreased. For 100% labeled AF-actin, the viscosity dropped to approximately half that of unlabeled actin, compared with the 100% ATR-actin which showed ~2 order of magnitude reduction in viscosity to ~5 cp. As a comparison, 5 cp was the approximate viscosity of non–column-purified actin (S&W-actin) prepared by our method. The reduction in viscosity was not due to a change in the polymer fraction because, by high shear viscometry (not shown), we measured a critical concentration of ~30 μg/ml for both ATR- and AF-actin, comparable with that measured by Tait and Frieden (1982*a*) and Wang and Taylor (1980), respectively. Additionally, variation in the purification of the labeled actin, from contaminating factors that decrease the actin viscosity, does not seem to be an issue because these results have been consistent in numerous preparations.

The diffusion coefficients measured by spot FPR for various ratios of labeled to unlabeled actin are shown in Table I and the fluorescence recovery traces in Fig. 3. Although the calculated diffusion coefficients varied between experiments, and there are limitations on the accuracy of diffusion coefficient calculations from such low recovery traces (see Discussion), we always found that ATR-actin traces recovered to a greater extent and had a higher calculated diffusion coefficient than AF-actin. There was only a slight increase in recovery in the spot FPR measurements with increasing percent label for both AF and ATR-actin, in apparent contrast to the FBV results which showed a dramatic decrease in viscosity with the percent labeled (Fig. 2). This illustrates the relative sensitivity and range of the assays.

Modulation-Detection Periodic-Pattern FPR

The diffusion coefficient of AF-actin was also measured by periodic-pattern FPR. Fig. 4 indicates the effect of increasing the monitoring beam power and the fraction bleached. Monitoring beam power is expressed as the irradiation intensity (power per area), whereas the fraction bleached is the fractional decrease in DC level between the prebleach and the immediate postbleach fluorescence signal. Increasing the monitoring power or increasing the percent bleach increased the measured diffusion coefficient of AF-actin. In another experiment, the fraction AF-actin (percent label) was varied between 5 and 50%. Increasing the percent label also increased the measured diffusion coefficient by 30–40-fold (Fig. 5). In contrast, changing the percent label had little effect on spot FPR recovery traces (Fig. 3). Typically measurements of AF-actin diffusion coefficients were $\sim 10^{-10}$ cm^2/s but when the monitoring beam power and the percent labeled actin were minimized, and intermittent monitoring was employed, values as low as 10^{-11} cm^2/s were measured.

In one experiment the sample (10 μM actin, 5% AF-actin) was photobleached and monitoring was postponed to assure that the pattern would dissipate in the absence of

TABLE I
DIFFUSION COEFFICIENTS OF LABELED ACTIN MEASURED BY GAUSSIAN SPOT FLUORESCENCE PHOTOBLEACHING RECOVERY

% Labeled actin	Normal*		Preirradiated‡		
	$D \times 10^{-10}$	Recovery	$D \times 10^{-10}$	Recovery	% Bleach due to preirradiation
ATR	cm^2/s	%	cm^2/s	%	
5	0.58	52	0.38	94	17
10	1.15	37	1.39	62	12
25	1.92	35	2.30	97	17
50	2.65	26	23.60	94	23
AF					
5	0.020	84	0.082	109	17
10	0.049	39	0.287	42	12
25	0.047	23	0.342	71	18
50	0.315	12	1.54	115	23

*The diffusion coefficients of F-actin solutions were measured by spot FPR, using a photobleaching dose of 292 and 32.8 W-s/cm^2 for ATR and AF-actin, respectively. Calculations were made by averaging 4–10 sample traces and fitting the data according to Materials and Methods. The absolute values for the diffusion coefficients and percent recoveries may not accurately represent the exact nature of the actin filaments due to limitations in fitting recovery data to such a small recovery (see Discussion). FPR traces are shown in Fig. 3.

‡F-actin was "preirradiated" by irradiating actin solutions with 2-mm diameter gaussian spot to obtain a dose of ~239 and 18.9 W-s/cm^2 for ATR and AF-actin, respectively. Standard spot FPR measurements were then made within the exposed areas which showed an arbitrary ~20% decrease in fluorescence intensity. The "percent bleach due to preirradiation" is the normalized fluorescence decrease due to preirradiation at the positions in which the FPR measurements were taken.

photodamage due to the monitoring beam. The pattern was examined for 10 s after 1, 2, and 3 h. The extent of pattern dissipation after 1 h corresponded to a diffusion coefficient of 2×10^{-11} cm^2/s; after 2 h the value determined was 1.2×10^{-11} cm^2/s; and after 3 h no detectable pattern remained.

Actin Purification: Viscosity Inhibitors

The actin was prepared as described in Materials and Methods, which included gel permeation chromatography on Sephacryl S300, which has been previously described (e.g.; MacLean-Fletcher and Pollard, 1980*a*; Zaner and Stossel, 1982). We found that fractions eluting immediately before the actin peak contained factors that drastically reduced the actin viscosity as measured by FBV (Fig. 6). The actin and viscosity inhibitor elution profile shown in Fig. 6 is comparable with previous reports (MacLean-Fletcher and Pollard, 1980*a*; Casella and Maack, 1987). It has been suggested that the contaminant may be cap $Z_{(36/32)}$, which has recently purified and characterized (Casella and Maack, 1987; Casella et al., 1986). We found that the main actin peak contained inhibitors on the leading edge of the peak as shown by a reduced viscosity (Fig. 6), and depending on how conservatively the fractions were chosen, the pooled actin viscosity could be greatly affected. In the experiments reported here, the pooled actin (Fig. 6) typically had a viscosity of ~1,500 cp at 0.5 mg/ml under the defined conditions. We also collected the main peak of the inhibitor activity and added it in various volumes to purified AF- and ATR-actin to observe the effects on the viscosity and diffusion coefficient. Fig. 7 shows that at 30% vol/vol viscosity inhibitors to actin, the viscosity of column-purified actin (10% fraction labeled) drops to a basal level of ~5 cp, which was approximately the viscosity of S&W-actin. The viscosities of both AF- and ATR-actin decreased in a nonlinear manner and in an identical manner for both labeled actins. In contrast, the measured diffusion coefficient increased in a linear manner (Fig. 7) by approximately one order of magnitude and over a range in which the viscosity was at a minimum plateau level. The measured diffusion coefficient of the S&W-actin was greater than the linearly extrapolated diffusion coefficient for 100% volume of viscosity inhibitors. This is understandable because the entire pool of viscosity inhibitors was not collected (Fig. 6). At all concentrations of inhibitors the ATR-actin had higher diffusion coefficients than AF-actin, however this difference was not apparent for the S&W-actin. The spot FPR traces of this experiment are shown in Fig. 8 for AF-actin (ATR-actin was comparable).

Irradiation Damage

We found that light irradiation of AF- and ATR-actin filaments could induce damage that was detected by FPR, FBV, and by SDS-PAGE. The FBV assay was performed by irradiating the capillaries containing polymerized actin with an expanded laser beam (see Materials and Methods). Fig. 9 shows the effect of irradiation on the viscosity of a range of AF-actin/unlabeled actin ratios. As the irradiation dose was increased (by increasing the time of irradiation) the viscosity decreased nonlinearly. The higher the percent labeled actin, the greater was the change in

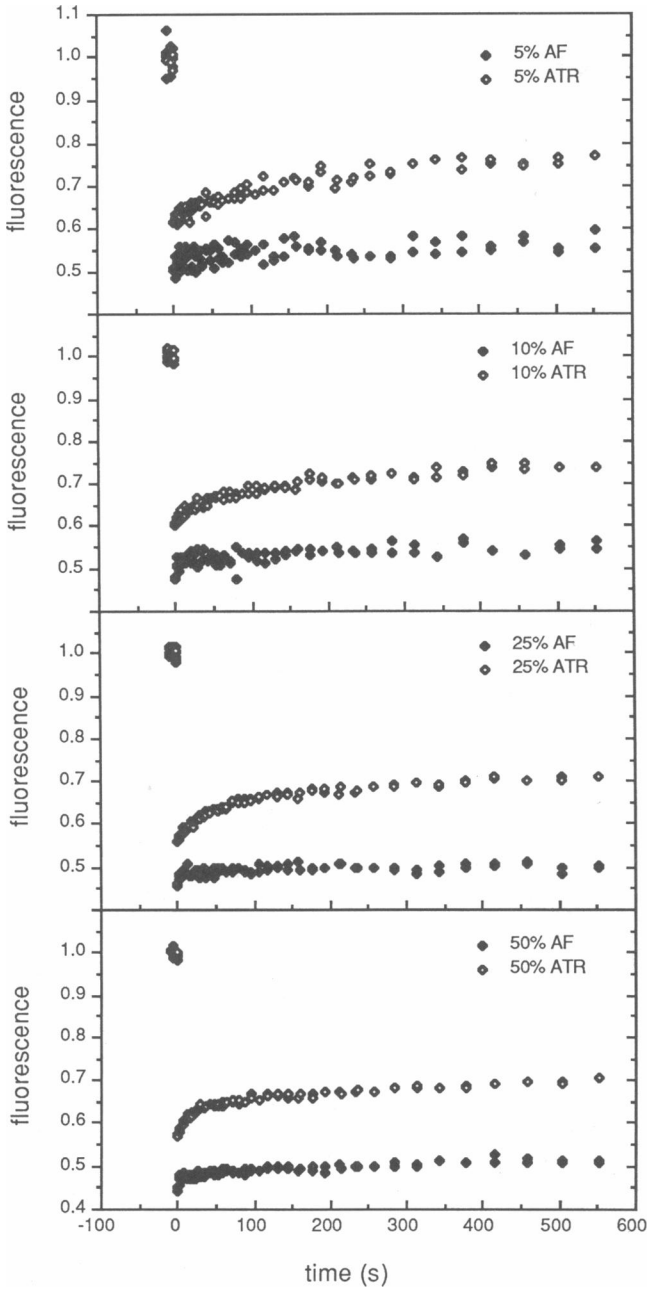

FIGURE 3 Fluorescence photobleaching recovery (FPR) traces of AF- and ATR-actin. AF- and ATR-actin at 0.5 mg/ml were photobleached at 488- and 514-nm wavelengths, respectively. The fluorescence recovery was monitored intermittently at increasingly long time intervals by regulating the monitoring beam shutter (see Materials and Methods). The spot size (w) was 2 μm and the fraction labeled actin is indicated. Each trace is an average of 4–10 sample monitors, and each was normalized to the prebleach fluorescence intensity.

viscosity. Unlabeled actin also showed a slight sensitivity to irradiation at 488 nm (Fig. 9) which, when tested at higher irradiation doses, proved to be about two orders of magnitude less sensitive than 5% labeled AF-actin. Unlabeled actin was also irradiated at 514 nm and no detectable decrease in viscosity was observed even at a dose of 800

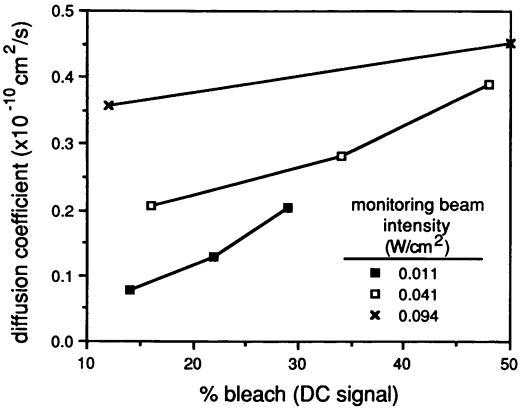

FIGURE 4 Periodic-pattern FPR: the effect of bleaching time and monitoring beam intensity on actin diffusion. Actin diffusion was measured by periodic-pattern FPR. Irradiation intensity (power per area) during recovery monitoring was varied as indicated by attenuating the laser beam. The percent bleach values due to the initial bleaching beam are given as the percentage decrease in the DC signal. Actin concentration was 0.75 mg/ml at 8% labeled AF-actin, ionic conditions were 100 mM KCl and 2.0 mM $MgCl_2$ and temperature at 23°C.

W-s/cm^2. Note also that the actin viscosity at zero irradiation dose decreased with increased percent label (Fig. 9), which is consistent with Fig. 2. The irradiation damage was also detected by spot FPR by irradiating a 2-mm diameter gaussian spot on FPR capillaries containing either AF- or ATR-actin, and then measuring the diffusion coefficient by spot FPR within the irradiated area. Diffusion was measured in area's with ~15–20% induced bleach (Table I). This irradiation caused a marked increase in the measured diffusion coefficient and percent recovery for both AF- and ATR-actin (Table I). The FPR traces are shown in Fig. 10 for ATR-actin. Note that the traces for nonirradiated ATR-actin showed only slight differences in the recovery curves with varying the percent labeled actin (Fig. 3) compared with the irradiated samples (Fig. 10).

The ability to recover from irradiation damage was assayed using FBV by allowing 5% ATR-actin samples to

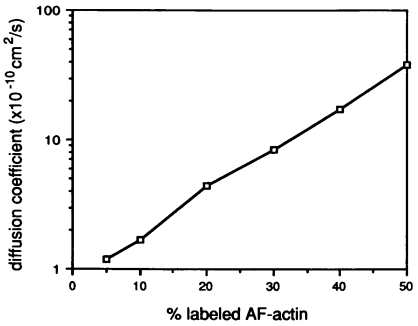

FIGURE 5 Periodic-pattern FPR: the effect of varying the fraction-labeled AF-actin. The fraction-labeled (percent label) AF-actin was varied from 5–50% as indicated and the diffusion coefficient was measured by periodic-pattern FPR. The actin concentration was 0.65 mg/ml, ionic conditions were 100 mM KCl and 0.2 mM $MgCl_2$ and temperature at 20°C.

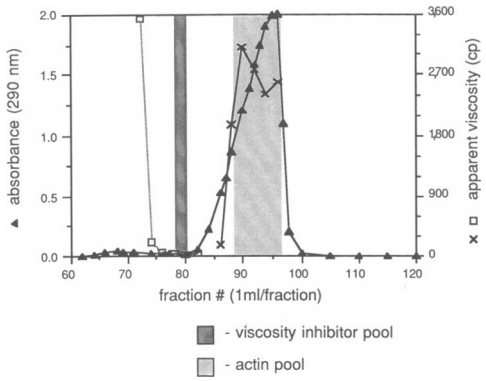

FIGURE 6 Column chromatography of actin. S&W actin (4 ml at 5 mg/ml) was applied to a 1.5 × 100 cm column of Sephacryl S-300 in buffer A at an elution rate of 14 ml/h. Fractions in the main peak were diluted to 0.5 mg/ml, polymerized, and the viscosity measured by FBV (*X*). Other fractions were assayed for viscosity inhibition activity by adding 33% vol/vol of a column fraction to 0.5 mg/ml pooled actin and measuring the viscosity by FBV (*open squares*). Shaded areas indicate the pooled fractions for actin and viscosity inhibitors.

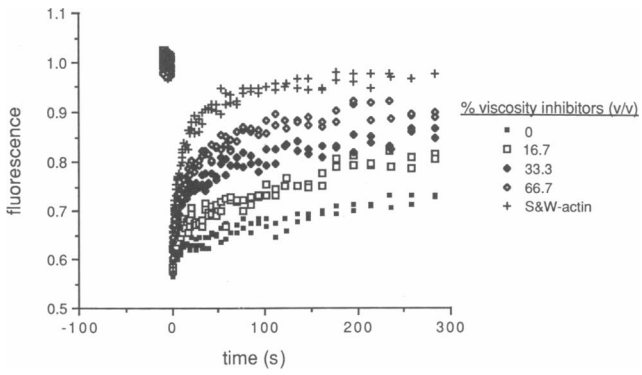

FIGURE 8 Effect of viscosity inhibitors on the FPR traces of AF-actin. Viscosity inhibitors were added to AF-actin (10% fraction labeled) and were photobleached as in Fig. 3. Also included is non–column-purified actin (S&W-actin) with 10% fraction labeled AF-actin. Fluorescence was normalized to prebleach fluorescence, and each recovery represents the average of nine or ten traces.

equilibrate for 6 h whereupon several capillaries were irradiated and either assayed immediately (within ~5 min), or allowed to incubate for 8 h and then assayed. The results shown in Fig. 11 indicate that the viscosity did not recover measurably in this time period. Identical results were found for AF-actin. Note also in Fig. 11 that a much higher irradiation dose was needed to induce damage to ATR-actin compared with AF-actin (Fig. 9). Recovery after irradiation damage was also assayed by spot FPR. AF-actin (10% labeled; 1 mg/ml actin) was preirradiated as in Fig. 10, and consistent with the FBV data, it exhibited only slight recovery after 11 h (data not shown).

Irradiation-induced covalent cross-linking of actin was detected by sedimentation followed by SDS-PAGE. AF- or ATR-actin was polymerized in capillaries and then subjected to various doses of irradiation. The contents of the capillaries were then sedimented and the supernatant and pellet were subjected to SDS-PAGE in the presence of 2-mercaptoethanol (described in Materials and Methods). The results for 10% AF-actin at 1 mg/ml are shown in Fig. 12. The pellet was composed predominately of the native actin species, but in addition species corresponding in molecular weight to actin dimers, trimers, and tetramers were found at a molar ratio of 1, 0.4, 0.1 (relative to dimers), respectively. Because the SDS-PAGE was performed under denaturing and reducing conditions, we believe that the high molecular weight species were actin monomers covalently cross-linked to form multimers. In the supernatant, which also contained cross-linked species, there was an increase in total protein above the measured actin critical concentration. At doses above 5 W-s/cm^2 (~5% bleach), the supernatant and pellet contained an increasing amount of material that would not enter a 7.5%

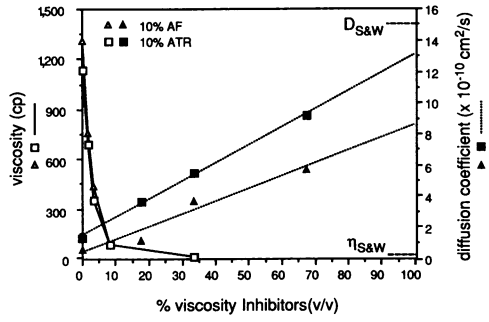

FIGURE 7 Effect of viscosity inhibitors on the diffusion and viscosity of actin. Actin viscosity inhibitors, obtained from actin column chromatography (see Fig. 6), were added to purified AF- and ATR-actin (10% fraction labeled) at the volumes indicated. The viscosity was measured by FBV and diffusion by FPR under the same conditions as Figs. 2 and 3, respectively. The viscosity and diffusion coefficient of non–column-purified actin (S&W-actin) are also included at extrapolated values of 100% viscosity inhibitors. Each FBV point represents the average of three samples, and the diffusion coefficients were obtained by fitting the average of nine or ten FPR traces. Actin concentration was 0.5 mg/ml.

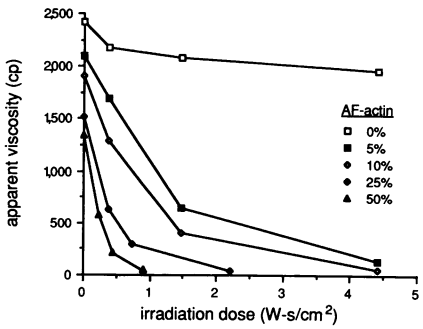

FIGURE 9 Effect of the fraction-labeled actin on the irradiation-induced decrease in AF-actin viscosity. AF-actin (0–50% fraction labeled) was polymerized in 100-μl glass capillary tubes and exposed to a 1.5 cm diameter (w = 0.75 cm) gaussian laser beam at 488 nm. The viscosity of the solution at 1 cm lengths within the exposed area was measured. The irradiation dose is defined as the laser intensity on the sample (power per area) multiplied by the time of irradiation. The irradiation intensity was 0.074 W/cm^2 and the measurement conditions were the same as Figs. 2 and 3.

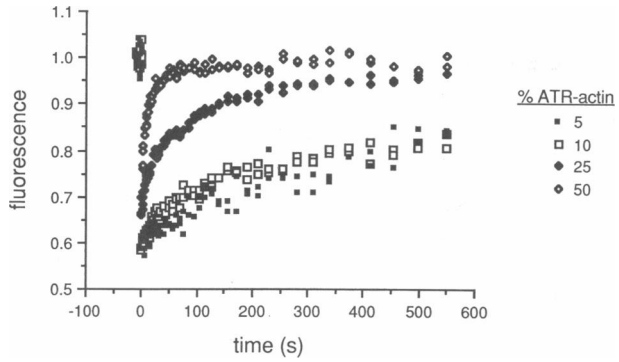

FIGURE 10 Effect of the fraction-labeled ATR-actin on irradiation-induced increase in FPR recovery. ATR-Actin (0–50% fraction-labeled) was polymerized in 200-μl-pathlength flat capillary tubes and exposed to a 2-mm diameter gaussian laser beam at 514 nm. The fluorescence recovery after photobleaching using a 2-μm spot (w) was then measured within the "preirradiated" area at positions which showed an average reduction in fluorescence of 17% (see Table I). The irradiation dose was 238.7 W-s/cm^2 (see Fig. 9), and the measurement conditions are the same as Fig. 2 and 3.

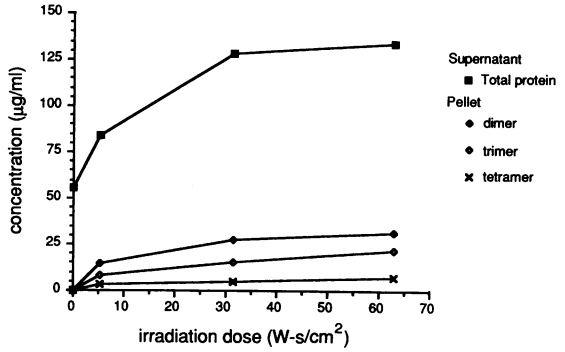

FIGURE 12 Sedimentation and cross-linking of irradiated AF-actin. AF-Actin (10% fraction labeled) was polymerized in 200-μl glass capillary tubes and irradiated by translating the tube longitudinally at a velocity of 14 cm/s in front of a 1.5 cm × 2 mm rectangular laser beam (488 nm) until the indicated dose was achieved. The contents of the tube were then placed into a centrifuge tube, allowed to incubate an additional hour, and sedimented at 100,000 g for 15 min. The supernatant was drawn off and protein content measured (*solid squares*). The pellet was resuspended, subjected to SDS-PAGE, stained with Coomassie Blue, and protein bands which were not present in the nonirradiated sample were quantitated by gel scanning. The irradiation-induced bands correspond by molecular weight to actin dimers (*solid diamond*), trimers (*open triangle*), and tetramers (x). Higher molecular weight material was detected at doses above 5 W-s/cm^2 but could not be quantiated due to technical limitations. Irradiation intensity was 0.37 W/cm^2 and actin concentration was 1 mg/ml.

gel, and thus could not be quantified due to technical limitations. The sum of dimer, trimer, and tetramer cross-linked material in the pellet was 25 μg/ml for a dose equivalent to a 5% bleach, whereas the total concentration of labeled actin in the sample was 100 μg/ml. Because 25 μg/ml cross-linked actin represents one-fourth of the labeled actin in the sample but only $\frac{1}{20}$ of the fluorophore was bleached, then at minimum 2.5 cross-links were created relative to each bleached fluorophore. This assumes that each cross-link is between two independent monomers, but the actual number of cross-links are greater if we consider the formation of multimeric species and redundant cross-links. The amount of dimer, trimer, and tetramer species increased nonlinearly with the irradiation dose and appeared to plateau at the highest doses shown (Fig. 12), but we note that the quantity of material too large to enter the gel also increased (not shown). ATR-actin showed similar results except approximately two orders of magnitude higher doses were needed to induce the same quantity of cross-links as the AF-actin. A complete titration of doses was not performed for the ATR-actin due to the technical difficulty of extremely long irradiation periods. Note that the dose of 5 W-s/cm^2 not only had an effect on covalent cross-linking, but also had a great effect on the FBV viscosity of AF-actin (Fig. 9). The effect of irradiation of G-actin solutions was also investigated. Four different concentrations were examined: solutions with total actin concentration of 10 μM were prepared with 0, 10%, and 40% AF-actin; the fourth solution had a total actin concentration of 24 μM, with 84% AF-actin. Samples were subjected to doses of 10 and 10^3 W-s/cm^2 in separate experiments, then the presence of covalently cross-linked oligomers was assayed using SDS-PAGE with ovalbumin as a standard. All actin samples migrated as a single species with molecular weight 43 kD. We conclude that any photoinduced cross-linking of G-actin under these conditions was below the limit of detection of the assay (<1%).

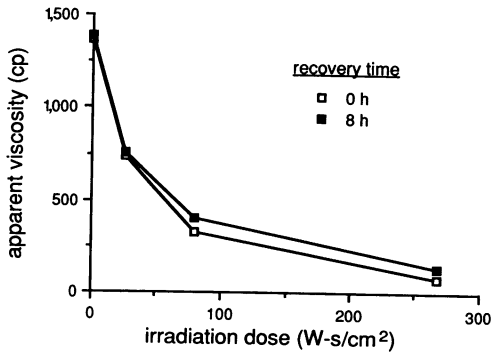

FIGURE 11 Lack of viscosity recovery after the irradiation-induced decrease in ATR-actin viscosity. ATR-Actin (5% fraction-labeled) was polymerized ~12 h in 100-μl glass capillary tubes and exposed to a 1.5 cm × 2 mm rectangular laser beam at 514 nm. The viscosity of the solution at 1-cm lengths within the exposed area was measured immediately after irradiation, or 8 h postirradiation. The irradiation intensity was 2.67 W/cm^2 and the measurement conditions were the same as Fig. 2.

The intensity of illumination (power per area) varied greatly between experimental protocols so it was critical to determine whether the photodamage depended upon dose rate as well as total irradiation dose. For example, in FPR measurements, the intensity ratio between the bleaching and monitoring beams was 7,500. Also, the intensity ratio between the FPR bleaching beam and the FBV irradiation

experiments was 250-fold or greater. We investigated this question by irradiating FBV capillaries containing 5% AF-actin at decreasing light intensities while increasing the time of irradiation to obtain identical total irradiation doses but at different rates. Over the two orders of magnitude in which the dose rate was changed, there was no measurable difference in the induced damage as shown in Fig. 13. However, the results of Fig. 13 cannot be necessarily extended to the 250-fold higher intensities encountered during an FPR photobleach.

We tested some compounds for the ability to reduce photodamage when added exogenously. Using FBV as an assay, we found that 50 mM reduced glutathione, 100 mM imidazole, and 1:2 phalloidin/actin molar ratio had no appreciable affect on irradiation-induced viscosity decrease of AF-actin. However 10 mM DTT had a slight protecting effect, whereas 50 mM DTT completely protected 10% AF-actin from photoinduced damage at dose of 4.5 W-s/cm^2. Using FPR as an assay, we found that 10% AF-actin with 50 mM DTT bleached as easily as without DTT, however the fluorescence recovered completely with a half-life of 2–3 s. This recovery time was independent of spot size (2 or 5 μm) which suggests that the fluorescence recovery was not a diffusive process. DTT had a similar protecting effect on 5% ATR-actin at a dose of 540 W-s/cm^2, however contrary to the AF-actin data, no fluorescence recovery was observed after 300 s recovery time. Potentially, FPR experiments can be performed in vitro with no photodamage under these conditions. In another experiment, the ability of rhodamine phalloidin to confer photosensitivity to unlabeled actin was tested. At a 1:4 rhodamine-phalloidin/actin molar ratio, the decrease in FBV viscosity with irradiation dose was similar to that in Fig. 11 (5% labeled ATR-actin). Therefore, rhodamine-phalloidin bound to actin caused damage to only one-fifth the extent of rhodamine on actin (as ATR-actin).

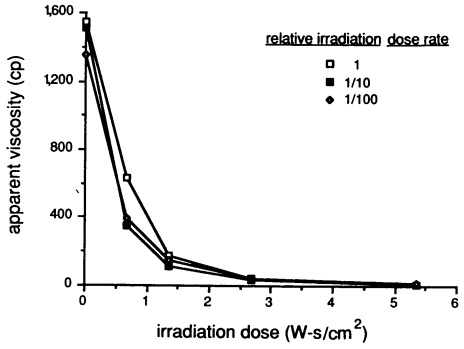

FIGURE 13 The effect of the irradiation dose rate on the viscosity of AF-actin. AF-Actin (10% fraction-labeled) was polymerized in 100-μl glass capillary tubes and exposed to a 1.5 cm × 2 mm rectangular laser beam at 488 nm. The irradiation was attenuated to 1/10 and 1/100 from 2.67 W/cm^2 while the time of irradiation was increased by 10 and 100, respectively. This corresponds to a two-order of magnitude change in dose rate while maintaining the same total irradiation dose. The viscosity measurement conditions are the same as Fig. 2.

DISCUSSION

Diffusion of Actin Compared with Previous Results

Previous measurements of F-actin diffusion coefficients have yielded contradictory results. Measurements using modulation-detection periodic-pattern FPR resulted in diffusion coefficients of 10^{-9}–10^{-10} cm^2/s (Lanni and Ware, 1984; Mozo-Villarias and Ware, 1984), whereas other investigators using gaussian spot FPR report diffusion coefficients of $<10^{-10}$ (Tait and Frieden, 1982*a*) and $\ll 2 \times 10^{-11}$ cm^2/s, or no recovery during the time course of the measurement (Tait and Frieden, 1982*b*; Doi and Frieden, 1984). Besides the differences in instrumentation, the previous periodic-pattern FPR measurements were made using non–column-purified actin (S&W-actin) with AF-actin as the tracer, whereas the gaussian spot experiments used column-purified actin and ATR-actin as the tracer. Our results indicate that both AF and ATR-actin are susceptible to irradiation-induced filament breakage, which increases the mobility of the filaments. ATR-actin, however, is five times less sensitive to breakage per percent fluorophore bleached than AF-actin (see below). Additionally, non–column-purified (S&W) actin prepared by our methods had a diffusion coefficient at least one order of magnitude greater than column-purified actin. There may be even more important consideration when comparing these diffusion coefficient measurements, and that is the difference in the geometry of the illumination in the two instruments as discussed below.

During a periodic-pattern FPR experiment, stripes are photobleached into the actin sample using a relatively large illumination beam. In our experiments the stripes had a period of 9.85 μm and the beam diameter was ~140 μm. The monitoring beam then illuminates this same area while the contrast of the photobleached pattern is observed to diminish. Although the monitoring beam is attenuated by about a factor of 5,000, the monitoring time is typically between 1,000 and 10,000 times greater than the bleaching time, so the total photon dose, which we have shown to be the operative criterion for photodamage at least at relatively low intensities (Fig. 13), is comparable. Therefore, we conclude that the initial bleach and the subsequent monitoring both contribute to the irradiation-induced shortening of actin filaments. Because periodic-pattern FPR measures the relaxation of the striped pattern, and all parts of the pattern are irradiated during the monitoring cycle, an aberrantly high diffusion coefficient is measured. This is consistent with Fig. 4, which demonstrates the dependence both on the percent bleach and the monitoring intensity. Even for the lowest percent bleach and the lowest monitoring intensity, the measured diffusion coefficient was still two to four times greater than the minimum values obtained when the monitoring beam was blocked intermittantly during recovery. A separate factor involving the illumination geometry is the selection of the pattern spac-

ing (k-vector). Filaments presumably have a broad range of filament lengths and thus of diffusion coefficients. The true form of the data is broadly multiexponential over several orders of magnitude. The average value reported thus depends upon the time window sampled and upon the time scale set by the k-vector. For example, parallel experiments on similar samples at several k-vectors (2,127 cm^{-1}, 4,254 cm^{-1}, and 6,381 cm^{-1}) showed a marked dependence of D on $1/k$ (not shown). Differences of nearly an order of magnitude in reported literature values of actin filament diffusion coefficients could be attributed to differences of the characteristic dimensions of the photobleached regions. These differences are complicated further by the differences in sampling bias between periodic pattern versus spot methods and by the fact that filament lengths may be considerably larger than the pattern periodicity and spot sizes employed.

Gaussian spot FPR also causes photodamage to labeled actin, however, diffusion coefficients are typically lower than those measured by periodic-pattern FPR. We can attribute this result to the difference in the illumination geometry between the two types of instruments. In the spot measurement, a gaussian spot is bleached and the fluorescence recovery into the same spot is monitored. Thus, damage is created within the spot, but this does not directly affect diffusion of fluorescence from outside of the bleached area because the areas surrounding the spot are not irradiated. This is consistent with the observation that the spot FPR recovery curves for 5–50% labeled actin (Fig. 3) are only slightly different, most likely due to intrinsic filament shortening with increased percent labeled actin (see Fig. 2), even though the susceptibility to photodamage greatly increases with the percent labeled actin (Figs. 9 and 10). Tait and Frieden (1982*b*) found that varying the bleach duration from 100 to 3,000 ms, which also increases the extent of photodamage, did not affect the measured rates of polymerization and immobilization of 5% ATR-actin. It can be argued that if filaments have a very low mobility and if bleaching a spot disrupts the filaments in that region, then spot FPR should show an initial post-bleach decrease in fluorescence. This would be due to shortened filaments within the spot diffusing out at a faster rate than the nonirradiated filaments in the surrounding areas diffuse in. This has not been observed in our experiments and the reasons are not directly evident. The shortened filaments diffusing out may contribute less to the fluorescent signal because they are maximally bleached, whereas the incoming filaments are minimally bleached and may also be less impeded due to the disruption of filaments in the bleached region. Data from Tait and Frieden (1982*b*) indicate a decrease in fluorescence after photobleaching actin but we do not know if this was due to the effect described above or, more likely, adventitious photobleaching during fluorescence monitoring.

An additional complication of the spot method for FPR studies of actin filament diffusion is that the spot size must be kept very small for recovery times to be within a reasonable range for reliable measurement. As we shall discuss later, the very low values for actin filament diffusion coefficients can be reasonably interpreted to mean that actin filaments are extremely long, perhaps hundreds of microns. The use of a spot size that may be two orders of magnitude smaller than the filament lengths means that fluorescence recovery could occur by segmental motion or orientational relaxation in addition to diffusion of the filament center of mass. However, the fact that diffusion coefficients measured by the spot technique are lower than those measured by the pattern technique using higher period spacings and much larger illumination spot sizes provides some indication that photodamage effects and sampling biases discussed in the previous and succeeding paragraphs are more important than the effects of local and orientational filament motions.

Our measured diffusion coefficients for AF and ATR-actin under various conditions of percent labeled actin and preirradiation times are given in Table I. Our work indicates that ATR-actin has a component with a diffusion coefficient in the range of 10^{-10} to 10^{-11} cm^2/s, but the major fraction has a lower diffusion coefficient of $<10^{-11}$ cm^2/s. When interpreting these data it is important to consider that the method of analysis we used (Yguerabide et al., 1982) determines the best fit of the data to a single diffusing species, yielding the diffusion coefficient and percent recovery. The calculated diffusion coefficient is a weighted average that is a function of the spot size, the intermittent monitoring beam gating interval, the total acquisition period, and the weight fractions of the actin filament lengths, because solutions of actin are not monodisperse (Kawamura and Maruyama, 1970), and the contribution of the fluorescent signal for each filament is dependent on its weight fraction rather than number fraction. Although it is difficult to derive an analytical weighting function, the contribution of the individual factors can be understood qualitatively. The spot size (w) determines the lifetime (τ_D) of a specific component with diffusion coefficient D ($=w^2/4\tau_D$) and, when combined with the other acquisition parameters, determines the range of diffusion coefficients that can be measured. In our case, $w \approx 2$ μm, so $\tau_D \approx 10^{-8}/D$ (e.g.; $\tau_D = 1{,}000$ s for $D = 10^{-11}$ cm^2/s). The analysis method relies upon the strong dependence of the linearity of the transformed data (see Yguerabide et al., 1982), $R(t) = [F(\infty)/(F(\infty) - F(t]$, on the value of $F(\infty)$, thus linearization of $R(t)$ is used to determine the value of $F(\infty)$. This strong linear dependence, however, does not hold for times $<\tau_D$, as can be seen in Fig. 3 of Yguerabide et al. (1982). Thus, a useful lower limit for acquisition times for this analysis method is $>\tau_D$. For lower signal to noise ratios though, acquisition times of 5–10 $\times$ τ_D may be necessary. If we choose a sampling rate of at least once per lifetime as the lower limit for sampling, and acquisition times of at least one lifetime, then the useful range of diffusion coefficients measurable

by our acquisition scheme (see Materials and Methods) is $1 \times 10^{-8} > D > 2 \times 10^{-11}$ cm^{2}s^{-1}. Using these criteria to measure a diffusion coefficient of $<10^{-12}$ cm^{2}s^1, our acquisition time should be >3 h. Other methods of analysis suffer from this same limitation. Tait and Frieden (1982*b*) for example use a nonlinear least squares fit to the first 16 terms of the series solution describing the recovery (Axelrod et al., 1976) to estimate τ_D. This method requires that the mobile fraction be known, estimated from the data, or determined by iterative techniques. To estimate the percent recovery, a minimum of one lifetime of data should be required, especially for lower signal to noise ratios.

Our work indicates that ATR-actin has detectable, albeit low diffusion coefficients (discussed above). This disagrees with previous in vitro studies using spot FPR which indicate zero fluorescence recovery after 36 s and that actin is completely immobile (Tait and Frieden, 1982*b*). We attribute this difference to several factors. First, the ATR-actin previously used was labeled with IATR containing a contaminant with an absorbance at 360 nm, most likely an intermediate of the rhodamine synthesis which was subsequently iodinated. We were able to partially purify this contaminant and it represented ~50% by weight (in two different lots) of the dye preparation. We infer by presence of an absorbance peak at 360 nm in the previously reported ATR-actin spectrum (see Fig. 1 of Tait and Frieden, 1982*a*) and the difference in the measured extinction coefficient of IATR (23,000 vs. 49,340 M^{-1} cm^{-1}), that ~50% of the ATR-actin preparation previously reported was contaminated with a covalently linked impurity. Arakawa and Frieden (1984) found that 60% labeled actin, which was probably only ~30% ATR-actin, had a relatively high diffusion coefficient of $\sim 1.5 \times 10^{-9}$ cm^2/s. In contrast, we found that 50% ATR-actin diffuses only slightly faster than 5% ATR-actin. Thus, the contaminating actin may have incurred this effect, however this is not consistent with their lower reported diffusion coefficients than ours at lower tracer levels. Second, we noted that Tait and Frieden (1982*b*) measured the time course of recovery for only 36 s. Little or no recovery should be seen for such a short monitoring period although they did mention that after 400 s zero recovery was observed. More importantly, their recovery traces showed a slight decrease in fluorescence during the 36-s recovery period. We postulate that adventitious bleaching of the sample during the monitoring period may have obscured a very slow fluorescence recovery. Alternatively, this could represent the initial decrease in fluorescence due to disruption of filaments as discussed above. In our measurements, the monitoring beam was gated such that we illuminated only during counting, and the sampling interval was increased (see Material and Methods) so as to minimize the number of illumination periods. Adventitious photobleaching for our measurements is calculated to be <3.5% for a total acquisition time of 600 s. We cannot give a single actin diffusion coefficient because the purity of the actin and probably the ionic conditions will affect the diffusion, but the ability to strictly limit adventitious bleaching is absolutely essential to detect such slow mobility. It is also conceivable that if we purified our actin to even greater extents (see Pardee and Spudich, 1982), we would observe essentially no fluorescence recovery. To test this proposal it would be essential to measure the recovery a very long time (i.e., many hours). We can state that column-purified actin has an extremely low average diffusion coefficient ($<10^{-11}$ cm^2/s), which varies according to the absolute purity of the actin and the method of measurement, and approaches or surpasses the lower limit of measurement by standard FPR techniques.

Photodamage

Photodamage or the general term "photodynamic action" has been observed in many biological systems (Spikes and Glad, 1964) including the following: the illumination of dichlorotriazinyl-fluorescein (DTAF)–labeled tubulin in vitro prevented assembly of tubulin (Leslie et al., 1984); illumination of fluorescein-labeled concanavalin A (Sheetz and Koppel, 1979) and fluorescein isothiocyanate-labeled erythrocyte ghosts and BHK membrane preparations (Lepock et al., 1978) caused covalent cross-linking of membrane proteins; addition of methylene blue or riboflavin-5′-phosphate caused trypsin activity to be photosensitive (Spikes and Glad, 1964). In addition, photosensitivity of actin has been observed: Lanni et al. (1981) have noted a photoinduced polymerization, measured by Airy-pattern spot FPR, at high-labeled/unlabeled AF-actin ratios; Martonosi and Gouvea (1961) observed photooxidation and filament depolymerization of actin in the presence of sensitizing dyes in solution. Whereas there are several mechanisms responsible for photodecomposition and photosensitization (Kasche and Lindqvist, 1964; Foote, 1968), in oxygenated systems the triplet state of the dye can provide energy for the production of singlet oxygen and other highly reactive species responsible for photofading and other oxidative reactions (Davidson and Trethewey, 1976; Oster et al., 1959; Kuramoto and Kitao, 1982; Foote, 1968). Thus, highly reactive species are not necessarily produced from photodecomposition, but are the cause of it. Such reactive species are probably responsible for the irradiation-induced covalent cross-linking of AF and ATR-actin (Fig. 12) and other fluorescently labeled proteins. The number of reactive species created by each photon of light absorbed, and the probability of photodecomposition are specific to each fluorophore and the surrounding conditions. Therefore, photobleaching is not strictly linked to photodamage, but in our experiments it provides a convenient reference point.

We have shown that both AF and ATR-actin are susceptible to photodamage. A primary effect of irradiation of labeled actin is breakage of actin filaments. This is inferred by the decrease in viscosity measured by FBV (Figs. 9, 11, and 13) and the increase in the diffusion

coefficient subsequent to irradiation (Table I, Fig. 10). There was not a direct correspondence between amount of bleaching and irradiation-induced damage between AF and ATR-actin. For example, in the FBV assay a dose of 4 vs. 270 W-s/cm^2 was required to bring AF and ATR-actin, respectively, to the same viscosity. This difference can be partly attributed to the suboptimal wavelengths used for excitation (488 vs. 495 nm for AF-actin, and 514 vs. 560 nm for ATR-actin). However, these doses correspond to a fluorescence bleach of ~5% for AF-actin and ~25% for ATR-actin. Therefore not only does ATR-actin require a higher illumination dose to bleach (~10-fold), but it can be bleached about five times greater than AF-actin before the same extent of filament damage occurs. Roughly the same result was seen in the SDS-PAGE cross-linking data. These observations are consistent with those of Johnson and Garland (1982) who reported a 10-fold greater dose requirement to achieve equivalent fluorescence depletion in tetramethylrhodamine compared to fluorescein at 514 and 488 nm, respectively. They also observed that fluorescein was much more susceptible to photodecomposition even under anaerobic conditions, whereas tetramethylrhodamine was stable under these conditions.

A second effect of irradiation of labeled actin is the covalent cross-linking of actin protomers within filaments. Our data indicates that multiple cross-links are formed relative to the decomposition of each fluorescein molecule (photodecomposition may not be strictly linked to cross-linking) and that cross-linking is mediated by some diffusible species. The fact that solutions of labeled G-actin did not form detectable levels of cross-linked species upon intense irradiation suggests further that the diffusible species responsible for cross-linking within F-actin either are produced only when the irradiated AF-actin is within a filament, or, more likely, are too shortlived to effect cross-linking of individually diffusing actin molecules. The photoinduced actin cross-links may act as "cappers" of filament ends preventing reannealing at actin filament breaks. This is inferred by the lack of recovery in the irradiation-induced reduction in actin viscosity even after 8 h postirradiation (Fig. 11), compared with mechanical disruption created by drawing the FBV ball through the capillary or sonication (Zaner and Stossel, 1982), which recovers in 2–3 h.

We have explored the possibility that local heating could play a role in the photodynamic damage. It is unlikely that local heating is involved for two reasons: (*i*) 50 mM DTT completely inhibited the damage to actin; and (*ii*) our estimate of local heating under the experimental conditions employed is negligible (see Appendix). Local heating has been addressed previously for other FPR experimental conditions (Axelrod, 1977; Lanni, 1981).

The fluorophores for both AF and ATR-actin are conjugated primarily to cys 374 on actin. It is important to determine if this site conveyed the irradiation sensitivity of labeled actin because fluorescent probes can be conjugated to other sites. We found that rhodamine-phalloidin caused unlabeled actin to become photosensitive, assayed by FBV (see Results). Because phalloidin is not covalently linked to actin, covalent linkage to cys 374 is not a prerequisite for photoinstability, and is also consistent with the interpretation (see above) that the damaging species is diffusible. This result does not preclude the possibility that phalloidin binds at or extremely close to cys 374.

Previous work has shown that certain compounds can inhibit bleaching of fluorophores and/or act as scavengers to photodecomposition byproducts (Bock et al., 1985; Picciolo and Kaplan, 1984; Leslie et al., 1984). We found that 50 mM reduced glutathione, 100 mM imidazole, or 1/2 phalloidin/actin did not prevent photodamage to labeled actin assayed by FBV, whereas 50 mM DTT effectively did inhibit damage. Picciolo and Kaplan (1984) found that DTT reduced fading of fluorescein isothiocyanate (FITC)–labeled rubella infected cells. We found that the 50 mM DTT did not inhibit or reduce photobleaching of AF- or ATR-actin, but in the case of AF-actin the fluorescence recovered with a half-life of 2–3 s independent of spot size (2 or 5 μm). This indicates that the recovery was not due to diffusion of fluorescent species, but may involve the formation of a nonfluorescent oxidized form of the fluorophore which subsequently was reduced by the DTT, although many other explanations are possible.

The relatively low diffusion coefficient of actin filament solutions could be explained by the diffusion of extremely long noninteracting rigid rods (Lanni and Ware, 1984), by steric constraints imposed by entanglement of long filaments (Zaner and Stossel, 1983; Ito et al., 1987), or by self-association of filaments via "weak" interactions (Sato et al., 1985). In all cases, there is a regime where filaments are predicted to have measurable diffusion coefficients which will decrease as functions of increasing filament length and concentration. We have produced a transition in the actin state, defined by a rapid change in viscosity, caused by modulating filament length using viscosity inhibitors (Fig. 7). Unfortunately, at this transition point the diffusion coefficient of the actin solution was extremely low, precluding reliable determination of the diffusion coefficient and fractional recovery by FPR technique employed. However, the nearly linear dependence of diffusion on the added volume of viscosity inhibitors (Fig. 7) seems to exclude the possibility of actin network formation as argued by Tait and Frieden (1982*b*). In fact, Janmey et al. (1986) argued that the nearly linear relationship between the diffusion coefficient and actin filament length modulated by the actin-binding protein "brevin," measured by Doi and Frieden (1984), was consistent with the theory that F-actin diffuses as long filaments restricted only by steric constraints.

If, as we surmise, the actin filaments are not immobilized by attractive forces, the magnitudes of the filament diffusion coefficients measured indicate that actin filaments formed from column-purified actin are much longer

than is conventionally presumed. If actin filaments are viewed as independent stiff rods, the relationship between number-average filament diffusion coefficient and number-average filament length L is (Lanni and Ware, 1984)

$$\langle D \rangle = \frac{kT}{3\pi\eta\langle L \rangle} [\ln (\langle L \rangle / w) - 0.09].$$

From this equation a D of 10^{-11} cm^2/s, using a filament width w of 8 nm, corresponds to a filament length of ~0.5 mm. If the filaments are viewed as interpenetrating stiff rods topologically constrained from orientational motion, the length estimate would be reduced by one third (Doi and Edwards, 1978). Because this length is even greater than the shortest dimension of our cuvettes, we do not believe that literal interpretation of this equation is warranted, but we do believe that very long filaments are formed in these solutions. For the higher diffusion coefficients observed as a result of photodamage, length estimates based on this equation can be used to estimate the probability of filament cleavage relative to a photobleaching event. From the data of Fig. 4 and of Table I we estimate that probability at between 10^{-2} and 10^{-3}.

We conclude that irradiation of AF- and ATR-action produces two principal artifacts. For each photobleaching event multiple cross-links between actin protomers within filaments are formed, and cleavage occurs at a lower probability. These artifacts place significant restraints on the use of fluorescent actin analogues to infer native actin behavior. For FPR experiments the cross-linking of protomers within filaments may not be a serious problem, because it does not alter the measured parameters directly. The cleavage of filaments clearly does affect the results of FPR measurements, as we have demonstrated. However, differences among literature values for actin filament diffusion coefficients may also be substantially attributable to other factors such as illumination geometry, sampling time, and purity of the actin preparations. The effects of photoinduced filament cleavage of FPR measurements are less consequential when the actin sample contains species that shorten filament length. In the design of FPR measurements of F-actin samples, photoinduced artifacts may be minimized by minimizing the fraction of labeled actin in the sample, the fraction of fluorescence photobleached by the bleaching pulse, the monitor beam intensity, and the monitor duty cycle. Selection of the dye and the site of labeling may also be important. We have shown that ATR-action has the advantage of being less susceptible than AF-action to photodamage but also has the inherent disadvantage of reduced native properties (as evidenced by lower viscosity and higher filament diffusion coefficients). We believe that for many actin experiments the advantages of the FPR measurement, principally the interpretability in terms of molecular assembly parameters and the absence of any mechanical perturbations, will continue to make it an attractive technique in comparison to the alternatives.

These results also have practical implications for fluorescence studies in living cells including the analyses of fluorescent protein analogues, inert volume tracers, and physiological indicators. Attention must be given to experiments designed to assess possible photoinduced artifacts, and to quantifying and reporting total illumination doses. The importance of minimizing illumination doses has been previously stressed (Bright and Taylor, 1986; Taylor et al; 1986). Methods that can minimize photobyproducts such as low-dose imaging, the development of new dyes (Waggoner, 1986), the implementation of photoactivatable fluorophores (Ware et al; 1986), and/or the utilization of improved labeling schemes may be the focus for future progress into this important field.

APPENDIX

Thermal Transient Due to High-Intensity Illumination of a Homogeneous Absorbing Solution

During the photobleaching phase of a FRAP experiment, a significant amount of energy is focused into a very small volume of matter. In the original application of the FRAP technique to the study of cell membrane fluidity, the absorption of light occurs at a surface embedded in an essentially nonabsorbing volume. Axelrod (1977) presented an analysis of membrane heating during photobleaching, and found that for a finite two-dimensional heat source in a three-dimensional medium, the local increase in temperature was bounded and, under the conditions of the experiment, insignificant. The calculation of the temperature field for a three-dimensional heat source such as the bulk specimens prepared for this study proceeds along similar lines, and is presented here for the Gaussian beam used in our experiments.

The excitation field in these experiments was an axially symmetric focused beam having a 2.0-μm radius waist over an axial range of ~20 μm. Because the specimen thickness was 200 μm, we make the conservative assumption for this calculation that the 2.0-μm beam actually extends through the specimen, so that there will be no axial heat flow. In fact, the defocused zones of the beam above and below the geometric flow provides another route for heat loss from the most intensely-irradiated volume. With the above conservative assumption, the temperature field in the solution therefore will have the cylindrical symmetry of the illumination field, and we have assumed that the absorbance is low enough so that dI/dz, the energy absorbed per unit axial distance, is constant through the sample.

Fourier's equation (Carslaw and Jaeger, 1947) specifies the relation between the temperature field, $v(\mathbf{r}, t)$, and the source field, $s(\mathbf{r}, t)$:

$$\partial v/\partial t = K\nabla^2 v + s, \tag{1}$$

where K is the thermal diffusivity of the material (here, $K \simeq$ thermal diffusivity of water). When the initial temperature field is a constant, $v(\mathbf{r}, 0) = v_0$, the homogeneous term in the integral solution is also constant, so that

$$v(\mathbf{r}, t) = v_0 + \int_0^t (4\pi K(t - t'))^{-3/2} \cdot \int_v s(\mathbf{r}', t') \exp\left\langle \frac{-|\mathbf{r} - \mathbf{r}'|^2}{4K(t - t')} \right\rangle d\mathbf{V}'\, dt'. \tag{2}$$

In this case, the source function is proportional everywhere to the photobleaching radiation field.

$$s(\mathbf{r}, t) = \begin{cases} 0, & t < 0 \\ s_0 \exp(-2\rho^2/w^2), & t \geq 0, \end{cases} \quad (3)$$

where $\rho^2 = x^2 + y^2$ is the radial cylindrical coordinate. A conservative assumption is that the source term is constant at every point during the photobleaching period, even though the absorbance of the solution decays significantly during this time due to photobleaching. The maximum increase in temperature occurs at the center of the radiation field, and is found by setting $\mathbf{r} = 0$.

$$\Delta v(\mathbf{r}, t) = \int_0^t (4\pi K t')^{-3/2} \int_v s(\rho') \cdot \exp\left(-\frac{|\rho - \rho'|^2 + (z - z')^2}{4Kt'}\right) dV'\, dt'$$

$$\Delta v(0, t) = \int_0^t \frac{1}{4\pi K t'} \int_0^\infty \int_0^{2\pi} s_0 \exp(-2\rho^2/w^2) \cdot \exp(-\rho^2/4Kt')\rho\, d\theta\, d\rho\, dt'$$

$$= \frac{s_0 w^2}{8K} \ln(1 + 8Kt/w^2). \quad (4)$$

Thus, it can be seen that there is a fundamental difference between the case analyzed by Axelrod and the three-dimensional absorber, where the temperature field diverges logarithmically with time. Under the conditions of a FRAP experiment, it must then be determined that, at a given absorbance and power, the duration of bleaching is short enough to keep Δv_{max} at an acceptable level. The source strength s_0 can be expressed in terms of the absorbance of the specimen and the peak intensity of the beam. A computation for typical experimental conditions is given below.

- P_0 Total beam power = 0.3 mW
- w Beam waist radius = 2.0 μm
- I_0 Central intensity of Gaussian beam = $2P_0/\pi w^2$ = 5,000 W/cm^2
- ϵ Dye extinction coefficient = 60,000 M^{-1} cm^{-1}
- c Dye concentration = 2.4×10^{-6} M
- l Specimen thickness = 0.02 cm
- A Absorbance = $\epsilon c l = 2.9 \times 10^{-3}$
- ΔI_0 Absorption rate = $I_0 A \ln(10)$ = 33.2 W/cm^2
- ρ_w Density of specimen $\simeq$ 1 g/ml (water)
- c_w Specific heat $\simeq$ 4.2 Joule/g° K (water)
- s_0 Source strength = $\Delta I_0/\rho_w c_w l$ = 394.7°K/s
- t_B 100 ms
- K_w Thermal diffusivity of water = 1.42×10^{-3} cm^2/s.

Using the above values in Eq. 4,

$$\Delta v(0, t_B) = (1.39 \times 10^{-3}) \ln(1 + 28{,}400.) = 0.014° \text{ K}.$$

The actual temperature rise is probably smaller than this due to heat loss through the surfaces of the optical cell, the decay of the absorbance, and radiation loss due to fluorescence, which occurs with a quantum efficiency of as much as 50%. Though we have used the specimen thickness (l) in the calculation of the absorbance (A) and source strength (s_0), we note that in the low-absorbance limit, which applies in this case, the dependence on l is normalized out in the calculation of s_0.

As can be seen from Eq. 4 Δv is an increasing function of beam size (w). Therefore we also compute Δv for the case where w = 20 μm at the same I_0 (P_0 = 30 mW):

$$\Delta v(0, t_B) = (0.139) \ln(1 + 284) = 0.79° \text{ K}.$$

These conservative calculations show that the expected thermal transient in our FRAP experiments is insignificant. The decay of this temperature field at the end of the bleaching period occurs with a time constant roughly given by $w^2/4K$ for short bleach periods, t_B for long bleach periods, or by $[l]^2/16K_G$ for window-limited heat loss when $t_B \gg [l]^2/4K_w$ [K_G = thermal diffusivity of glass). One unexplored possibility that would significantly increase heating would be absorbance of protein molecules in the specimen at the dye excitation wavelength. While the strong ultraviolet absorbance of protein is well known, weak absorbance in the blue part of the spectrum can be inferred from inactivation during prolonged irradiation of solutions of purified unlabeled actin and other proteins. We have no evidence at this time of any significant effect in FRAP experiments of this weak protein absorbance. Nonlinear optical processes that occur under intense irradiation could in principle increase the transient absorbance of a protein solution, but there is no evidence for this mechanism operating here. Finally, as noted in this report, the protective effect of antioxidants suggest that there is no thermal component to photoinduced damage.

We appreciate the technical assistance of Judy Montibeller, Chris Thompson, and Steve McDonough for the preparation of the actin. We gratefully acknowledge many helpful suggestions by Dr. Lauren Ernst, and critical reading of the manuscript by Dr. Ernst and Drs. Gary Bright and Len Pagliaro.

This work was supported by grants from the National Science Foundation (DMB-8607843) to Dr. Ware, and National Institutes of Health (AM-32461-04 and GM-34639) to Dr. Taylor.

Received for publication 22 December 1987 and in final form 30 June 1988.

REFERENCES

Axelrod, D. 1977. Cell surface heating during fluorescence photobleaching recovery experiments. *Biophys. J.* 18:129–131.

Axelrod, D., D. E., Koppel, J. Schlessinger, E. Elson, and W. W. Webb. 1976. Mobility measurements by analysis of fluorescence photobleaching recovery kinetics. *Biophys. J.* 16:1055–1069.

Arakawa, T., and C. Frieden. 1984. Interaction of microtubule-associated proteins with actin filaments. Studies using the fluorescence-photobleaching recovery technique. *J. Biol. Chem.* 259:11730–11734.

Bock, G., M. Hilchenbach, K. Schauenstein, and G. Wick. 1985. Photometric analysis of antifading reagents for immunofluorescence with laser and conventional illumination sources. *J. Histochem. Cytochem.* 33:699–705.

Bradford, M. M. 1976. A rapid and sensitive method for the quantitation of microgram quantities of protein utilizing the principle of protein-dye binding. *Anal. Biochem.* 72:248–254.

Bright, G. R., and D. L. Taylor. 1986. Imaging at low light level in fluorescence microscopy. *In Applications of Fluorescence in the Biomedical Sciences.* D. L. Taylor, A. S. Waggoner, R. F. Murphy, F. Lanni, and R. R. Birge, editors. Alan R. Liss, Inc., New York. 257–288.

Carlson, F. D., and A. B. Fraser. 1974. Dynamics of F-actin and F-actin complexes. *J. Mol. Biol.* 89:273–281.

Carslaw, H. S., and J. C. Jaeger. 1947. Conduction of Heat in Solids. Oxford University Press, Oxford, UK.

Casella, J. F., and D. J. Maack. 1987. Cap$Z_{(36/32)}$ is a contaminant and the major inhibitor of actin network formation in conventional actin preprations. *Biochem. Biophys. Res. Commun.* 145:625–630.

Casella, J. F., D. J. Maack, and S. Lin. 1986. Purification and initial characterization of a protein from skeletal muscle that caps the barbed ends of actin filaments. *J. Biol. Chem.* 261:10915–10921.

Davidson, R. S., and K. R. Trethewey. 1976. The role of the exicted singlet state of dyes in dye sensitized photooxygenation reactions. *J. Am. Chem. Soc.* 98:4008–4009.

Doi, M., and S. F. Edwards. 1978. Dynamics of rod-like macromolecules in concentrated solution. *J. Chem. Soc. Faraday Trans.* 274:560–570 (part 1), 918–932 (part 2).

Doi, Y., and C. Frieden. 1984. Actin polymerization. The effect of brevin

on filament size and rate of polymerization. *J. Biol. Chem.* 259:11868–11875.

Foote, C. S. 1968. Mechanisms of photosensitized oxidation. *Science (Wash. DC).* 162:963–970.

Fowler, V. M., and H. B. Pollard. 1982. In vitro reconstitution of chromaffin granule-cytoskeleton interactions: ionic factors influencing the association of F-actin with purified chromaffin granule membranes. *J. Cell. Biochem.* 18:295–311.

Fowler, V., and D. L. Taylor. 1980. Spectrin plus band 4.1 cross-link actin. Regulation by micromolar calcium. *J. Cell Biol.* 85:361–376.

Ito, T., K. S. Zaner, and T. P. Stossel. 1987. Nonideality of volume flows and phase transitions of F-actin solutions in response to osmotic stress. *Biophys. J.* 51:745–753.

Janmey, P. A., J. Peetermans, K. S. Zaner, T. P. Stossel, and T. Tanaka. 1986. Structure and mobility of actin filaments as measured by quasielastic light scattering, viscometry, and electron microscopy. *J. Biol. Chem.* 261:8357–8362.

Johnson, P., and P. B. Garland. 1982. Fluorescent triplet probes for measuring the rotational diffusion of membrane proteins. *Biochem. J.* 203:313–321.

Kasche, V., and L. Lindqvist. 1964. Reactions between the triplet state of fluorescein and oxygen. *J. Phys. Chem.* 68:817–823.

Kawamura, M., and K. Maruyama. 1970. Electron microscopic particle length of F-actin polymerized in vitro. *J. Biochem.* 67:437–457.

Koppel, D. E.,D. Axelrod, J. Schlessinger, E. L. Elson, and W. W. Webb. 1976. Dynamics of fluorescence marker concentration as a probe of mobility. *Biophys. J.* 16:1315–1329.

Kuramoto, N., and T. Kitao. 1982. Contribution of singlet oxygen to the photofading of some dyes. *J. Soc. Dyers Colour.* 98:334–340.

Lanni, F. 1981. Development and application of fluorescence photobleaching techniques for the study of cytoplasmic motility. Ph.D. thesis. Harvard University, Cambridge, MA.

Lanni, F., and B. Ware. 1982. Modulation detection of fluorescence photobleaching recovery. *Rev. Sci. Instrum.* 53:905–908.

Lanni, F., and B. R. Ware. 1984. Detection and characterization of actin monomers, oligomers, and filaments in solution by measurement of fluorescence photobleaching recovery. *Biophys. J.* 46:97–110.

Lanni, F., D. L. Taylor, and B. R. Ware. 1981. Fluorescence photobleaching recovery in solutions of labeled actin. *Biophys. J.* 35:351–364.

Lepock, J. R., J. E. Thompson, and J. Kruuv. 1978. Photoinduced crosslinking of membrane proteins by fluorescein isothiocyanate. *Biochem. Biophys. Res. Commun.* 85:344–350.

Leslie, R. J., W. M. Saxton, T. J. Mitchison, B. Neighbors, E. D. Salmon, and J. R. McIntosh. 1984. Assembly properties of fluorescein-labeled tubulin in vitro before and after fluorescence bleaching. *J. Cell Biol.* 99:2146–2156.

MacLean-Fletcher, S., and T. D. Pollard. 1980*a*. Identification of a factor in conventional muscle actin preparations which inhibits actin filament self-association. *Biochem. Biophys. Res. Commun.* 96:18–27.

MacLean-Fletcher, S. D., and T. D. Pollard. 1980*b*. Viscometric analysis of the gelation of *Acanthamoeba* extracts and purification of two gelation factors. *J. Cell Biol.* 85:414–428.

Martonosi, A., and M. A. Gouvea. 1961. Studies on actin. V. Chemical modification of actin. *J. Biol. Chem.* 236:1338–1344.

Mozo-Villarias, A., and B. R. Ware. 1984. Distinctions between mechanisms of cytochalasin D activity for Mg^{2+} and K^{+}-induced actin assembly. *J. Biol. Chem.* 259:5549–5554.

Mozo-Villarias, A., and B. R. Ware. 1985. Actin oligomers below the critical concentration detected by fluorescence photobleaching recovery. *Biochemistry.* 24:1544–1548.

Oster, G., J. S. Bellin, R. W. Kimball, and M. E. Schrader. 1959. Dye sensitized photooxidation. *J. Am. Chem. Soc.* 81:5095–5099.

Pardee, J. D., and J. A. Spudich. 1982. Purification of muscle actin. *Methods Enzymol.* 85:164–181.

Picciolo, G. L., and D. S. Kaplan. 1984. Reduction of fading of fluorescent reaction product for microphotometric quantitation. *Adv. Appl. Microbiol.* 30:197–234.

Plank, L., and B. R. Ware. 1986. Assembly of *Acanthamoeba* actin in the presence of *Acanthamoeba* profilin measured by fluorescence photobleaching recovery. *Biochem. Biophys. Res. Commun.* 140:308–312.

Plank, L., and B. R. Ware. 1987. *Acanthamoeba* profilin binding to fluorescein-labeled actins. *Biophys. J.* 51:985–988.

Pollard, T. D., and J. A. Cooper. 1982. Methods to characterize actin filament networks. *Methods Enzymol.* 85:211–233.

Sato, M., G. Leimbach, W. H. Schwarz, and T. D. Pollard. 1985. Mechanical properties of actin. *J. Biol. Chem.* 260:8585–8592.

Sheetz, M. P., and D. E. Koppel. 1979. Membrane damage caused by irradiation of fluorescent concanavalin A. *Proc. Natl. Acad. Sci. USA.* 76:3314–3317.

Simon, J. R., and D. L. Taylor. 1986. Preparation of a fluorescent analog: acetamidofluoresceinyl-labeled *Dictyostelium discoideum* α-actinin. *Methods Enzymol.* 134:487–507.

Spikes, J. D., and B. W. Glad. 1964. Photodynamic action. *Photochem. Photobiol.* 3:471–487.

Spudich, J. A., and S. Watt. 1971. The regulation of rabbit skeletal muscle contraction. *J. Biol. Chem.* 246:4866–4871.

Tait, J. F., and C. Frieden. 1982*a*. Polymerization-induced changes in the fluorescence of actin labeled with iodoacetamidotetramethylrhodamine. *Arch. Biochem. Biophys.* 216:133–141.

Tait, J. F., and C. Frieden. 1982*b*. Polymerization and gelation of actin studied by fluorescence photobleaching recovery. *Biochemistry.* 21:3666–3674.

Taylor, D. L., J. Reidler, J. A. Spudich, and L. Stryer. 1981. Detection of actin assembly by fluorescence energy transfer. *J. Cell Biol.* 89:362–367.

Taylor, D. L., P. A. Amato, P. L. McNeil, K. Luby-Phelps, and L. Tanasugarn. 1986. Spatial and temporal dynamics of specific molecules and ions in living cells. *In* Applications of Fluorescence in the Biomedical Sciences D. L. Taylor, A. S. Waggoner, R. F. Murphy, F. Lanni, and R. R. Birge, editors. Alan R. Liss, Inc., New York. 347–376.

Waggoner, A. S. 1986. Fluorescent probes for analysis of cell structure, function, and health by flow and imaging cytometry. *In* Applications of Fluorescence in the Biomedical Sciences. D. L. Taylor, A. S. Waggoner, R. F. Murphy, F. Lanni, and R. R. Brige, editors. Alan R. Liss, Inc., New York. 3–28.

Wang, Y.-L., and D. L. Taylor. 1980. Preparation and characterization of a new molecular cytochemical probe: 5-iodoacetamidofluorescein-labeled actin. *J. Histochem. Cytochem.* 28:1198–1206.

Wang, Y.-L., F. Lanni, P. L. McNeil, B. R. Ware, and D. L. Taylor. 1982. Mobility of cytoplasmic and membrane-associated actin in living cells. *Proc. Natl. Acad. Sci. USA.* 79:4660–4664.

Ware, B. R., L. J. Brvenik, R. T. Cummings, R. H. Furukawa, and G. A. Krafft. 1986. Fluorescence photoactivation and dissipation (FDP). *In* Applications of Fluorescence in the Biomedical Sciences. D. L. Taylor, A. S. Waggoner, R. F. Murphy, F. Lanni, and R. R. Brige, editors. Alan R. Liss, Inc., New York, 141–157.

Yguerabide, J., J. A. Schmidt, and E. E. Yguerabide. 1982. Lateral mobility in membranes as detected by fluorescence recovery after photobleaching. *Biophys. J.* 39:69–75.

Zaner, K. S., and T. P. Stossel. 1982. Some perspectives on the viscosity of actin filaments. *J. Cell Biol.* 93:987–991.

Zaner, K. S., and T. P. Stossel. 1983. Physical basis for the rheological properties of F-actin. *J. Biol. Chem.* 258:11004–11009.